



Electrochemical deposition of a hydroxyapatite layer onto the surface of porous additively manufactured Ti₆Al₄V scaffolds

Radka Gorejová^a, Renáta Oriňaková^{a,b,*}, Zuzana Orságová Králová^a, Tibor Sopčák^c,
Ivana Šišoláková^a, Marek Schnitzer^{d,e}, Miroslav Kohan^d, Radovan Hudák^d

^a Department of Physical Chemistry, P. J. Šafárik University in Košice, Moyzesova 11, 040 01 Košice, Slovakia

^b Centre of Polymer Systems, University Institute, Tomas Bata University in Zlín, Trída Tomáše Bati, 5678 76001 Zlín, Czech Republic

^c Institute of Material Research, Slovak Academy of Science, Watsonova 47, 040 01 Košice, Slovakia

^d Department of Biomedical Engineering and Measurement, Technical University in Košice, Letná 9, 042 00 Košice, Slovakia

^e Biomedical Engineering s.r.o., Popradská 56/D, 040 11 Košice, Slovakia

ARTICLE INFO

Keywords:

Porous titanium
Additive manufacturing
Ceramic coating
Hydroxyapatite
Electrochemical deposition

ABSTRACT

Successful acceptance of biomaterials by a patient's body significantly depends on an interaction between the surface and the biological components of the host environment. In the case of orthopedic scaffolds, surface treatment may improve their osseointegration. This study deals with the electrochemical deposition of ceramic hydroxyapatite (HAp) coatings onto additively manufactured titanium specimens with a porous structure. The specimens of three different types (pore sizes of 200, 400, and 600 μm) were modeled using CAD software and fabricated using the Ti₆Al₄V titanium alloy. HAp coatings were electrochemically deposited onto the surface of un-annealed specimens using four different experimental conditions. Based on the results and optimization of the conditions with the un-annealed specimens, ideal conditions were selected for the coating of the annealed specimens. The nature of the ceramic layer on un-annealed and annealed samples was compared. Surface morphology and distribution of ceramic coatings on the surface of the specimens were compared and evaluated by scanning electron microscopy (SEM), X-ray diffraction (XRD), and energy-dispersive X-ray spectroscopy (EDX). The un-annealed specimens exhibited more compact surfaces and larger deposits of nanocrystalline HAp when compared to the annealed specimens. The results indicate that electrochemical deposition is a suitable method for the production of a ceramic coating layer onto the surface of porous titanium specimens with promising potential for clinical applications.

1. Introduction

Pure titanium and titanium alloy (Ti₆Al₄V) are among the most frequently used materials in biomedicine [1,2]. They exhibit a low weight (compared to steels), and high strength, they are corrosion resistant and biocompatible, hence they are optimal for applications in implantology (for hard tissue replacements in particular) [3]. The current trend in the field of hard tissue replacements lies in the development of materials with enhanced osteointegration in combination with the materials that exhibit required mechanical properties similar to those of the replaced parts of a human body [4]. By adjusting the implant surface properties, it is possible to achieve optimal bone-to-implant integration since the nature of the implant surface affects the adhesion of osteoblasts to an implanted material. The factor that is very

important for successful bone tissue ingrowth into an implant is the material porosity. In porous structures, pore sizes that are optimal for osteointegration vary, and while some of the literature sources state that the ideal pore size ranges from 100 μm to 400 μm [5,6], others propose the ideal pore size of 650 μm to 1400 μm [7]. The porous structure of implants is therefore of crucial importance in orthopedic tissue engineering [8,9] as it facilitates anchorage through the ingrowth of mineralized tissue into implant pores. There are multiple studies describing the effects of a porous structure on mechanical properties. An article by Murr et al. [10] describes the optimization of a porous structure in Ti₆Al₄V implants. The authors examined the effect of the geometry of individual pores on the mechanical properties of a porous material, and they found out that when they increased porosity from 59 % to 88 %, elastic modulus decreased from 3.03 to 0.58 GPa. Their

* Corresponding author at: Department of Physical Chemistry, P. J. Šafárik University in Košice, Moyzesova 11, 040 01 Košice, Slovakia.

E-mail address: renata.orinakova@upjs.sk (R. Oriňaková).

<https://doi.org/10.1016/j.surfcoat.2022.129207>

Received 4 November 2022; Received in revised form 20 December 2022; Accepted 23 December 2022

Available online 2 January 2023

0257-8972/© 2023 Elsevier B.V. All rights reserved.

findings have proved that the elastic modulus of metal implants may be reduced by implementing a porous structure. A similar study [11] deals with designing a spongy porous structure with 50 % porosity for bone tissue replacements. It has been confirmed that not only the percentage but also the distribution and morphology of pores significantly affect the mechanical properties of the materials and tissue ingrowth.

The coating of titanium alloys with bioceramics is also thoroughly studied [12–16]. In a study by Li et al. [17] authors investigated the deposition of HAp + TiO₂ ceramic coatings and performed a cross-sectional analysis using the electron probe microanalyzer. Results have shown that annealing at 650 °C led to the formation of cracks in the HAp coating or between the substrate and the deposited coating. Based on the observations of the microstructure, it has been concluded that an addition of TiO₂ to a HAp coating may efficiently enhance and reinforce the entire coating on the surface of titanium substrates. A similar study on the application of a HAp coating on a Ti substrate has been published by Hae-Won et al. [18]. They applied HAp coating by the sol-gel method. HAp layer exhibited the typical apatite phase at 400 °C, and the intensity of the apatite phase increased at a temperature of 450 °C and higher. The sol-gel layers of HAp and TiO₂ were applied with thicknesses of approximately 800 and 200 nm. The strength of the coating increased as a result of adding a TiO₂ layer when compared to the direct application of a HAp layer on a Ti substrate. The highest achieved coating strength was 55 MPa after thermal treatment at 500 °C.

The fabrication and surface finishing of objects made of titanium and titanium alloys affect the coating process as well [19–21]. Fabrication of porous structures using a titanium material by applying the selective laser melting (SLM) technology was carried out in a study by Taniguchi et al. [22]. They evaluated the effect of pore size on in vivo bone ingrowth in rabbits into porous titanium implants, while the pore sizes were 300, 600, and 900 μm. The quality of the fabricated implants was evaluated using microfocus X-ray computed tomography. Results of their analysis showed the average pore sizes of 309, 632, and 956 μm which can be caused by powder grain size. However, the authors stated that despite certain inaccuracies, all of the implant types exhibited a good bone-implant fixation ability. Specimens with a porous structure were also successfully fabricated by the additive manufacturing technique by Li et al. [23]. They produced porous structures using the Ti₆Al₄V material, and their results have proved that the selected technology did not affect in vitro tests as the biocompatibility and non-toxicity of the material were confirmed. They also confirmed that the porous structure eventually interconnected with the tissue which was also demonstrated by in vivo tests (beneficial effect of cell attachment and their proliferation). Kuboki et al. [24] have proved that with a pore size of 300 to 400 μm the implantation of porous HAp scaffolds in rats exhibited higher activity of alkaline phosphates, higher contents of osteocalcin, and better bone ingrowth. However, another study [5] described the implantation of 300 μm, 600 μm, and 900 μm porous Ti scaffolds produced by additive manufacture. The study aimed to detect the level of ingrowth between scaffolds and rabbit shin bone. In this case, the results show significantly higher bone ingrowth in 600 and 900 μm scaffolds than in 300 μm scaffolds.

The present study deals with the electrochemical deposition of ceramic hydroxyapatite (HAp) coatings onto titanium specimens with a porous structure which were fabricated by additive manufacturing. Materials with three different pore sizes (200, 400, and 600 μm) were prepared. Some of the samples undergo heat treatment before the coating application (annealed), while the other remained un-annealed. Several experimental approaches were used during the electrochemical deposition process to select the ideal coating conditions. Ti₆Al₄V specimens were subjected to investigation of their surface morphology and distribution of the ceramic coating using scanning electron microscopy (SEM), X-ray diffraction (XRD), and Energy-dispersive X-ray spectroscopy (EDX). The deposition of hydroxyapatite on the surface of titanium was studied, however, the electrochemical deposition on these types of structures (with a large pores) and its

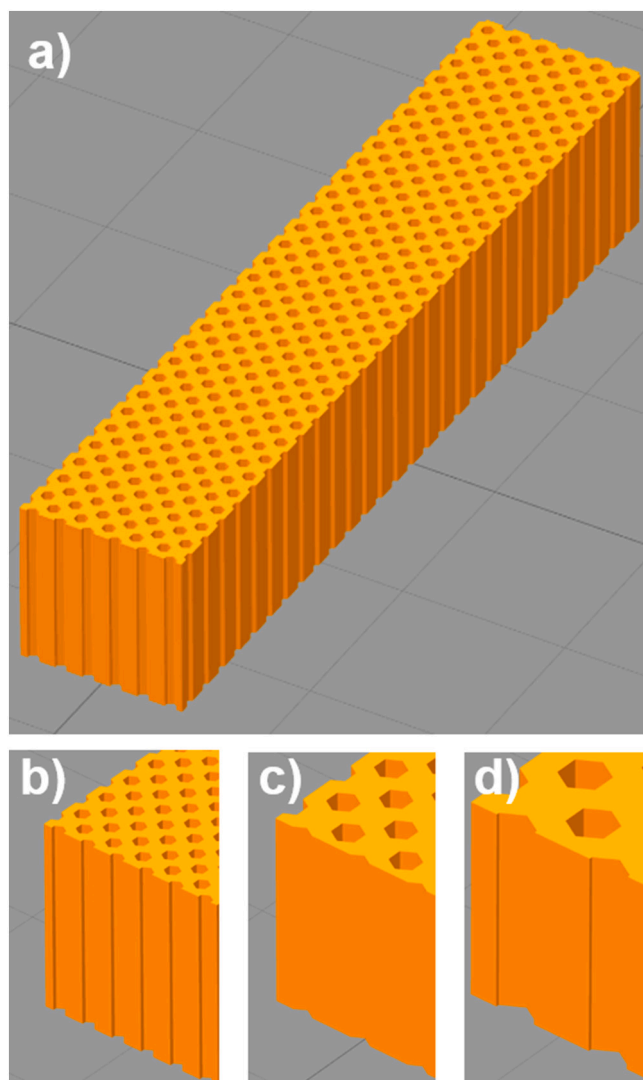


Fig. 1. Resulting design of the experimental samples. a: Total experimental sample with 200 μm pore size; b: detail view of the experimental sample with 200 μm pore size; c: detail view of the experimental sample with 400 μm pore size; d: detail view of the experimental sample with 600 μm pore size.

evaluation has not been widely documented yet.

2. Material and methods

2.1. Design of experimental specimens

Experimental specimens were designed in Solidworks 2019 software (Massachusetts, USA), where a three-dimensional rectangular object sized 5 × 5 × 25 mm was created. The design of the experimental samples was divided into three versions according to the size of the pores. The first version had a pore size of 200 μm, the second version 400 μm, and the third version 600 μm (Fig. 1). The porous structure of the experimental specimens was designed in Meshmixer software (Autodesk, Inc., USA). The resulting design was saved in STL format for further processing and fabrication of the specimens.

2.2. Additive manufacturing of Ti₆Al₄V scaffolds

The experimental specimens were manufactured using the Ti₆Al₄V powder with a grain size that ranged from 45 to 100 μm. The powder composition was as follows: Ti (90 %), Al (6 %), V (4 %), and other

Table 1
Basic 3D printing parameters.

Parameter	Value
Layer thickness	25 [μm]
Print speed	1–5 [cm^3/h]
Laser type and power	Fibre laser [100 W]
Scanning speed	7 m/s
Operating temperature	15–30 °C
Material used	Ti ₆ Al ₄ V

Table 2
Experimental conditions used in the process of optimizing the process of coating the un-annealed Ti₆Al₄V specimens with a HAp layer.

Method	Etching	Deposition time	Experimental deposition mode	Addition of hydrogen peroxide	Applied current/applied potential
O1	–	40 min (65 °C)	Galvanostatic	–	5 mA
O2	60 min in 1 M H ₂ SO ₄ at 60 °C	40 min (65 °C)	Galvanostatic	–	5 mA
O3	60 min in 1 M H ₂ SO ₄ at 60 °C	20 min (60 °C)	Potentiostatic	–	–0.8 V
O4	60 min in 1 M H ₂ SO ₄ at 60 °C	40 min (65 °C)	Galvanostatic	1 ml/1 35 % H ₂ O ₂	5 mA

components N, C, H, Fe, and O (<1 %). The additive technology, i.e. Selective Laser Sintering (SLS) was applied to fabricate specimens with various pore sizes. In this case, the Mlab 3D printer (Concept Laser, Germany) was used. Table 1 contains the basic technical parameters for

the fabrication of the experimental specimens.

The 3D printing process was followed by removing the support structure from the structure of experimental samples manually using spliers. Experimental samples were split into 2 groups (annealing samples and non-annealing samples). The group of annealing samples was subjected to the Nabertherm N 7/H annealing and hardening furnace with heat radiation (Nabertherm, Germany). The process of annealing and heating the experimental specimens were implemented gradually. In the first stage, the annealing furnace was heated to 300 °C for 90 min, then argon was supplied to the furnace for 150 min, and the furnace was heated to 820 °C. This temperature was maintained for 150 min. After this period elapsed, the temperature began to decrease to a value of 350 °C. Subsequently, the experimental specimens were taken out from the annealing furnace.

2.3. Electrochemical deposition of hydroxyapatite coating onto the porous specimens

The surface of the titanium specimens with a porous structure was coated with ceramic hydroxyapatite (HAp, Ca₅(OH)(PO₄)₃) using the electrochemical deposition method. To identify optimal deposition conditions, the un-annealed specimens were initially tested in several experimental procedures (marked as O1–O4). Based on the results obtained during the optimization stage, the experimental procedure that led to the deposition of HAp layers with the best physical and chemical properties was selected.

The surfaces of all titanium specimens were cleaned ultrasonically before the electrochemical deposition for 10 min in acetone, then in 96 % ethanol, and distilled water. In three of the four procedures (O2, O3, and O4), the cleaning was followed by the surface etching by immersing the specimens in 1 M sulphuric acid (H₂SO₄) at a temperature of 60 °C for 60 min to enhance the roughness of the specimen surface for better adhesion of the coating to the surface of the titanium specimens. Subsequently, the specimens were immersed in a beaker containing distilled water and cleaned ultrasonically for 30 min. The etching and cleaning

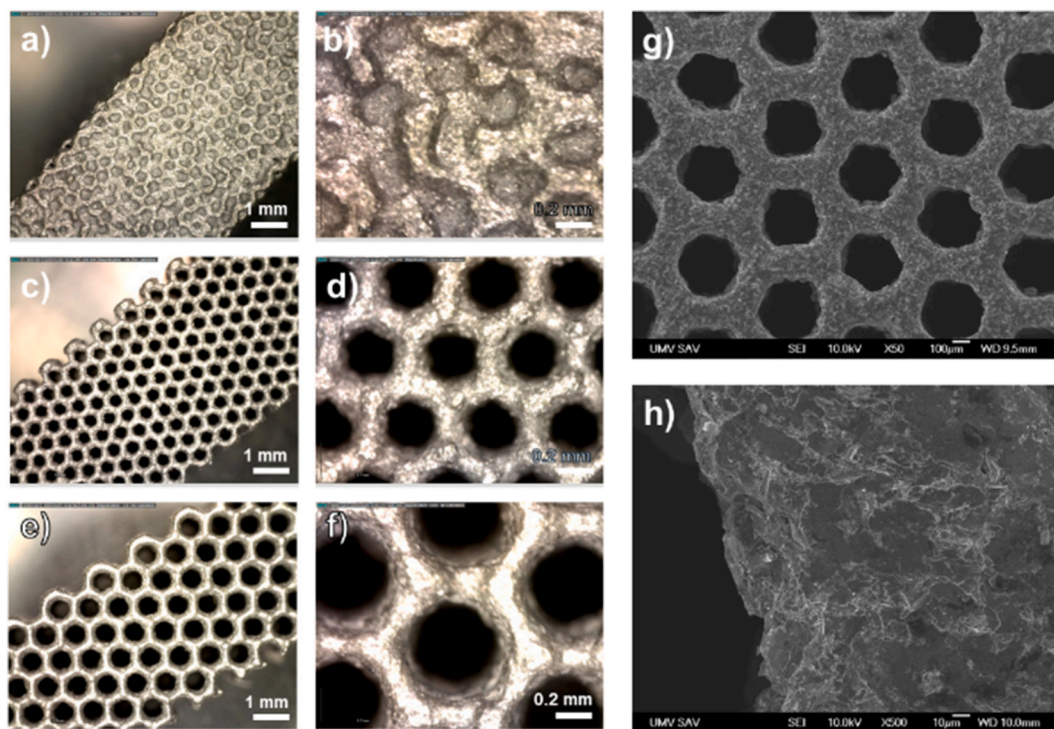


Fig. 2. Macroscopic images of the un-annealed specimens: (a) 200 μm at 50 \times magnification, (b) 200 μm at 200 \times magnification, (c) 400 μm at 50 \times magnification, (d) 400 μm at 200 \times magnification, (e) 600 μm at 50 \times magnification, (f) 600 μm at 200 \times magnification. SEM images of the un-annealed specimens (400 μm) without a coating: (g) at 50 \times magnification, (h) at 1000 \times magnification.

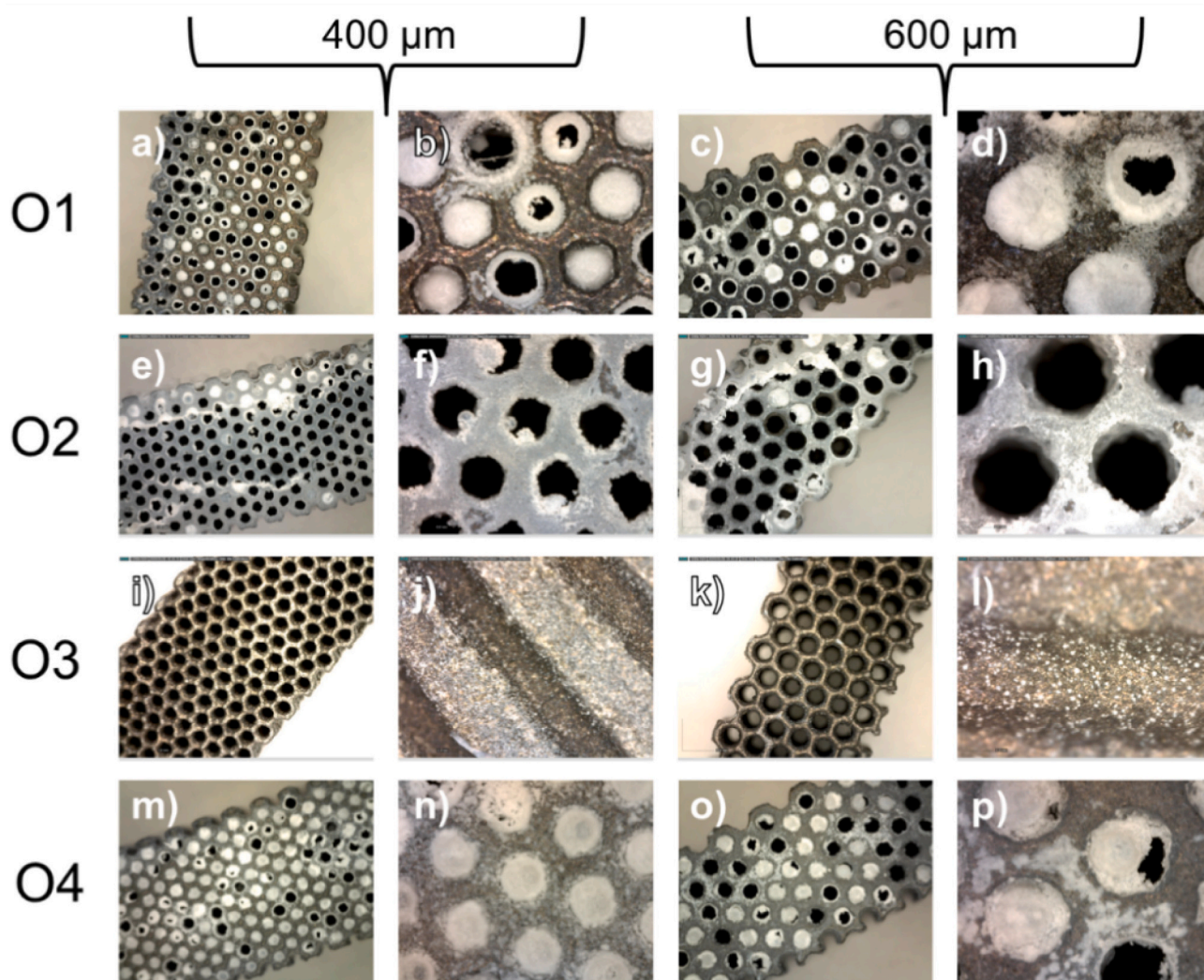


Fig. 3. Macroscopic images of the un-annealed specimens coated with a ceramic HAp layer by applying methods O1–O4: (a, e, i, m) 400 μm at 50 \times magnification, (b, f, j, n) 400 μm at 200 \times magnification, (c, g, k, o) 600 μm at 50 \times magnification, (d, h, l, p) 600 μm at 200 \times magnification.

steps were followed by drying in the air for 24 h.

Electrochemical deposition of the bioceramic layer onto the surface of the samples was carried out using Autolab M204 multichannel potentiostat with an FRA module (Metrohm AG, Herisau, Switzerland). The specimens were used as a working electrode, Ag/AgCl/KCl (3 mol/l) as a reference electrode, and Pt was used as a counter electrode. The solution that was used for the deposition of the HAp layer consisted of 2.5×10^{-2} mol/l of $\text{NH}_4\text{H}_2\text{PO}_4$ and 4.2×10^{-2} mol/l of $\text{Ca}(\text{NO}_3)_2$ [25].

The coating was carried out in the galvanostatic/potentiostatic mode with a constant current of 5 mA or a constant potential of 0.8 V for 20/40 min at a temperature of 65 ± 0.5 °C. The experimental conditions that were used during the optimization of the deposition conditions are summarised in Table 2. After the coating, the specimens were immersed in 1 M NaOH for 60 min at 65 °C and then thoroughly rinsed with distilled water and dried at 80 °C for the next 120 min. Obtained HAp coatings were not heat-treated after the deposition. To inhibit the formation of gaseous hydrogen, increase crystallinity, and enhance the morphology and microstructure of the HAp coatings, 1 ml/l of 35 % hydrogen peroxide was added to the electrolyte solution (O4) [26,27].

2.4. Characterization of the HAp-coated specimens

The surface morphology of the uncoated and coated specimens and

the chemical and phase compositions of ceramic coatings were studied and evaluated.

Macroscopic examination of the surface of titanium specimens was carried out using the Dino-Lite Premier AM4013MT digital microscope (1.3 MP, 200 \times magnification, Dino-Lite, Netherlands). Macroscopic images were made at 50 \times and 200 \times magnification. The characterization of the surface morphology was carried out using scanning electron microscopy (SEM, Jeol Ltd., Japan) and energy-dispersive X-ray spectroscopy (EDX, Inca, Japan). The specimens were weighed before and after the application of the ceramic layer to identify the weight of the deposited HAp coating.

The phase composition of the surface was examined by applying X-ray diffraction (XRD) and using the Philips X'Pert Pro diffractometer (Cu K α radiation, 40 kV, 50 mA, 2 θ between 10 and 90°, Philips, Netherlands).

3. Results and discussion

3.1. Surface morphology and structure of the un-annealed un-coated $\text{Ti}_6\text{Al}_4\text{V}$ specimens

The images of titanium specimens with a designed porous structure with a pore size of 200 μm (Fig. 2a and b) show that the SLS method did

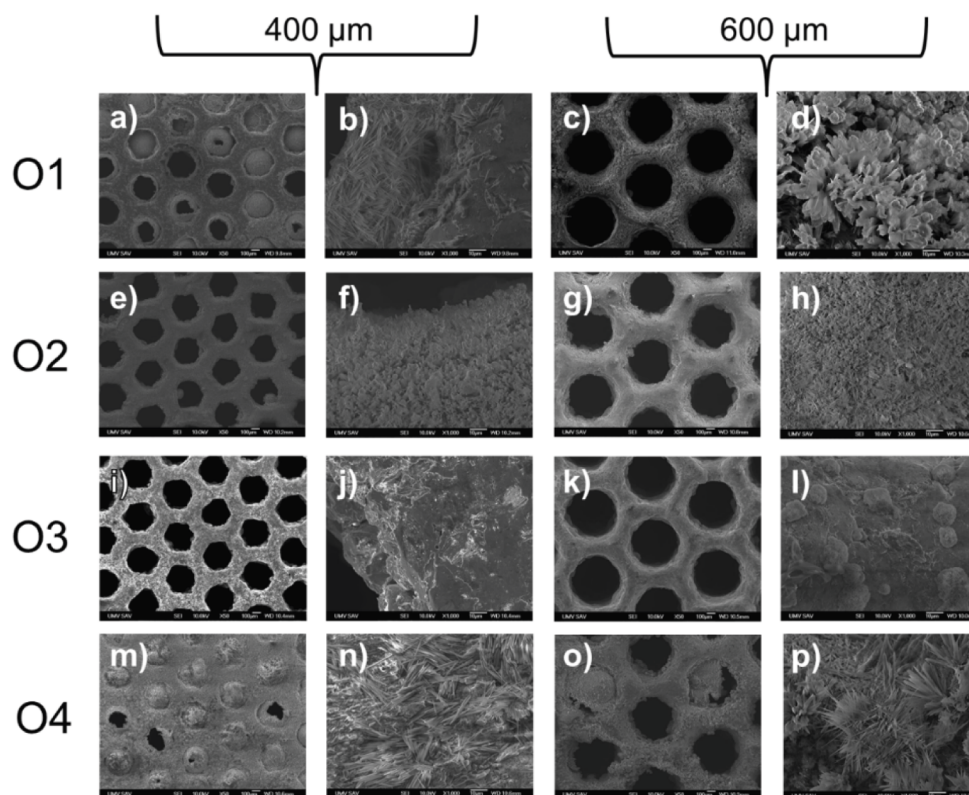


Fig. 4. SEM images of the un-annealed specimens coated with a ceramic HAp layer by applying the O1–O4 methods: (a, e, i, m) 400 μm at 50 \times magnification, (b, f, j, n) 400 μm at 200 \times magnification, (c, g, k, o) 600 μm at 50 \times magnification, (d, h, l, p) 600 μm at 200 \times magnification.

not facilitate creating pores of the required size. The surface exhibited a porous structure, but the pores remained closed. The reason why the required porous structure was not achieved may lay in the limitations of the used SLS technology. Therefore, the specimens with this pore size were not subjected to further analysis. Fig. 2c and d shows the images of specimens with a pore size of 400 μm while Fig. 2e and f shows the images of specimens with a pore size of 600 μm . The individual cells in the material are regular and correspond to the proposed design. Fig. 2g and h shows the representative SEM images of the surface of un-annealed titanium specimens without a HAp coating, where the irregularities of the uncoated surface may be seen (Fig. 2h).

The SLS technology is capable of creating porous structures for better osteointegration, nevertheless, it also exhibits certain limitations [29–31], which may explain the closed pores in the structure of the experimental specimens with a pore size of 200 μm . The main limiting factors of the selected manufacturing technology include the laser power, the size of the laser beam, titanium powder particle size, and conductivity around the material [32–34]. This has also been confirmed by the fact that the titanium powder used in the manufacture of the experimental specimens exhibited a particle size of 45–100 μm , which may cause closed pores in structures with a pore size of 200 μm in manufacturing experimental specimens. According to Liu et al. [35], when the solidification point is achieved rapidly, a metal layer created by SLS may enhance the force that binds it with the particles in the powder; however, it has been demonstrated that the specimens with defects on their surface might have enhanced the strength of the bond between the ceramic and the metal components. A study by Zhang et al. [36] described the fabrication of porous $\text{Ti}_6\text{Al}_4\text{V}$ implants with a composite HAp coating while using the SLS technology. They successfully fabricated a porous implant with a pore size of 400 μm . Based on an analysis of this porous structure, they concluded that the pore size of this structure was approximately 400 μm , but several partially molten particles of titanium powder adhered to the inner wall while the diameters

of these particles were approximately 25 μm . This result correlates with the result of our study.

3.2. Morphology, chemical, and phase compositions of the surface of un-annealed coated Ti-HAp specimens

A digital microscope was used to obtain microscopic images of the specimens at 50 \times and 200 \times magnifications (Fig. 3). A scanning electron microscope was used to acquire images showing a detailed microstructure of the surface of the deposited ceramic coating (Fig. 4).

As for the specimens fabricated using the O1 method, the ceramic layer was deposited unevenly (Fig. 3a–d) and the surface of the specimens was not homogeneously coated (Fig. 3a). The coating was concentrated around the pores whereas in farther areas it was inhomogeneous. An SEM analysis confirmed the deposition of HAp which was concentrated mainly inside the pores (Fig. 4a). As a result of this finding, the surface of the specimens was etched in sulphuric acid (1 M, 60 min. at a temperature of 65 $^{\circ}\text{C}$) before further coating to increase the roughness of the substrate and achieve a more homogeneous deposition of the HAp layer.

The analysis of specimens fabricated by the O2 method (Figs. 3e–h, 4e–h) shows that the surface of the specimens is not covered with a continuous coating layer even though the etching was performed. Some areas remain uncoated (Fig. 3e–g) because of the formation of gaseous H_2 during electrochemical deposition. In the process, gas bubbles were covering some areas on the specimen surface and thus prevented access to the electrolyte solution and therefore the deposition of HAp. To eliminate the undesired bubble formation on the surface of the working electrode, hydrogen peroxide (35 % H_2O_2 , 1 ml/l) was added to the electrolyte solution in the next step.

In addition to the methods that used a constant current (galvanostatic modes), a method with a constant potential was also tested (potentiostatic mode) (O3). However, when the O3 method was used,

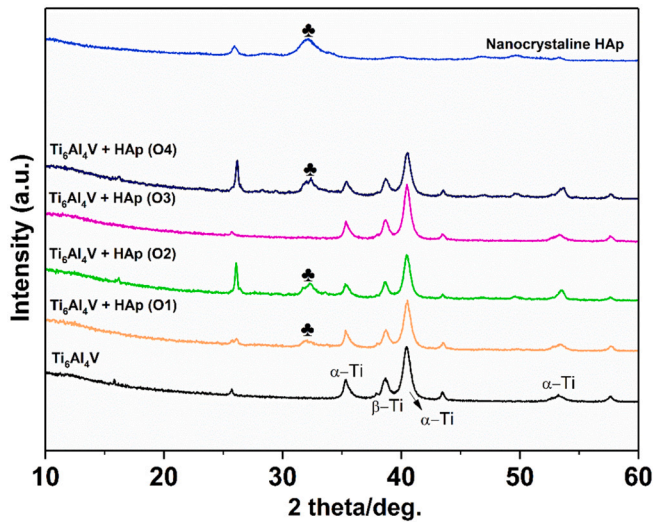


Fig. 5. XRD analysis of Ti_6Al_4V specimens coated with a HAp layer prepared via different electrochemical methods (O1–O4).

HAp deposition onto the surface of the Ti substrate did not occur (Figs. 3i–l), 4i–l). When compared to the other specimens, HAp crystals were not present at the surface (Fig. 3j–l) and pores were not filled with the ceramic layer. Although the surface of the specimens was etched before the deposition process, the resulting layer was not deposited and the XRD analysis did not prove the presence of nanocrystalline HAp (Fig. 5). This may be attributed to the fact that the potentiostatic mode with a predefined value of the potential of 0.8 V (selected based on the literature) during the deposition was not optimal for the deposition of a homogeneous layer of HAp onto Ti, and hence further deposition only occurred in the galvanostatic mode, which has proven to be a more suitable option.

The coating layer which was deposited by applying the O4 method (Figs. 3m–p, 4m–p) uniformly and evenly covered all areas of the specimens. It was deposited not only on the surface but also in the pores of the specimens. The HAp that was deposited on the surface of the specimens by the O4 method was spindle-like shaped (Fig. 4n, p) and this treatment was assessed as the most appropriate method for the next steps of the experimental procedure.

The XRD analysis (Fig. 5) revealed the presence of nanocrystalline HAp in all the studied samples, except for the case when the O3 method was used. With O1, O2, and O4 methods, the presence of a

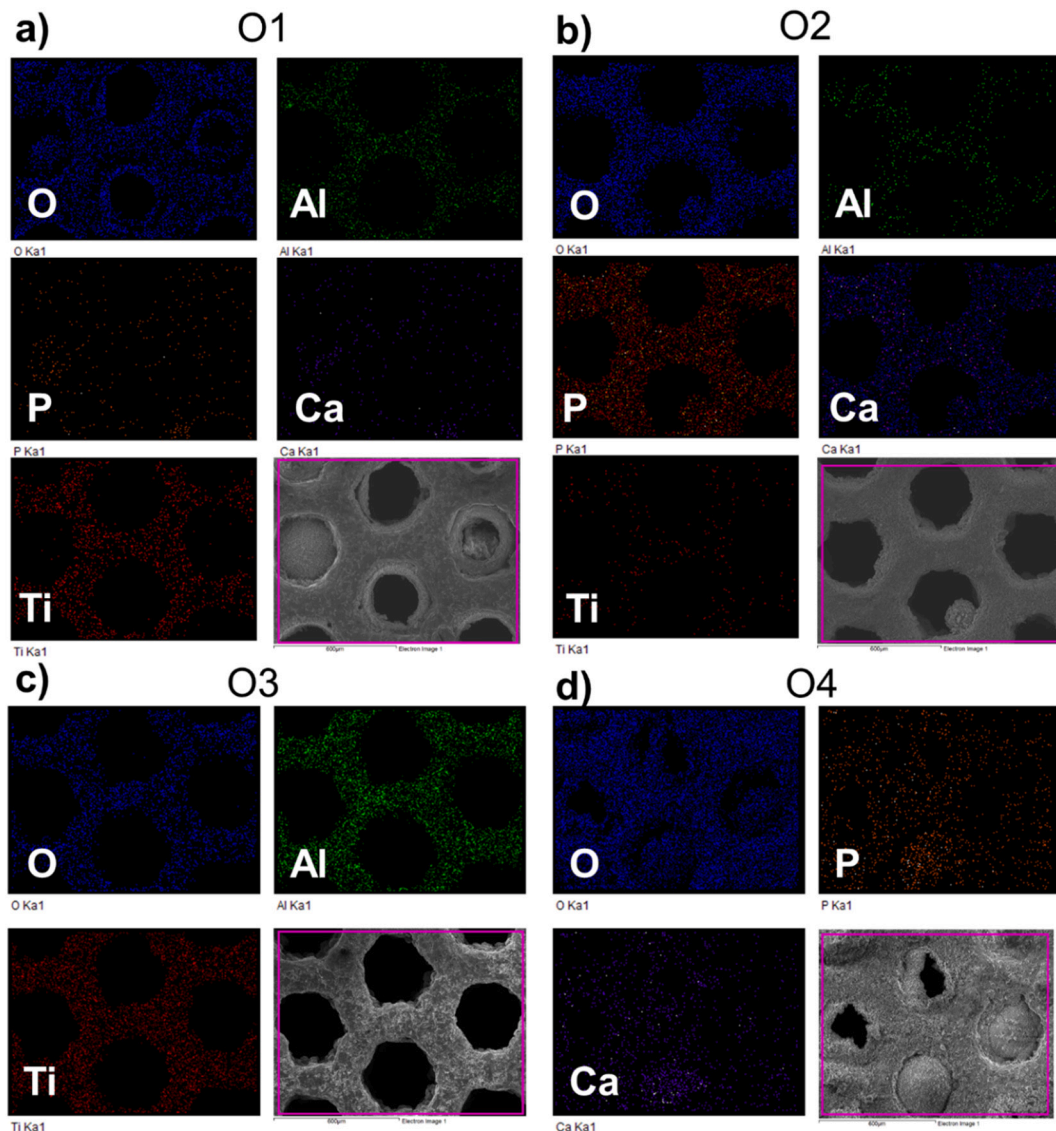


Fig. 6. EDX surface analysis of the un-annealed specimens coated with a ceramic HAp layer prepared by the electrochemical methods (O1–O4).

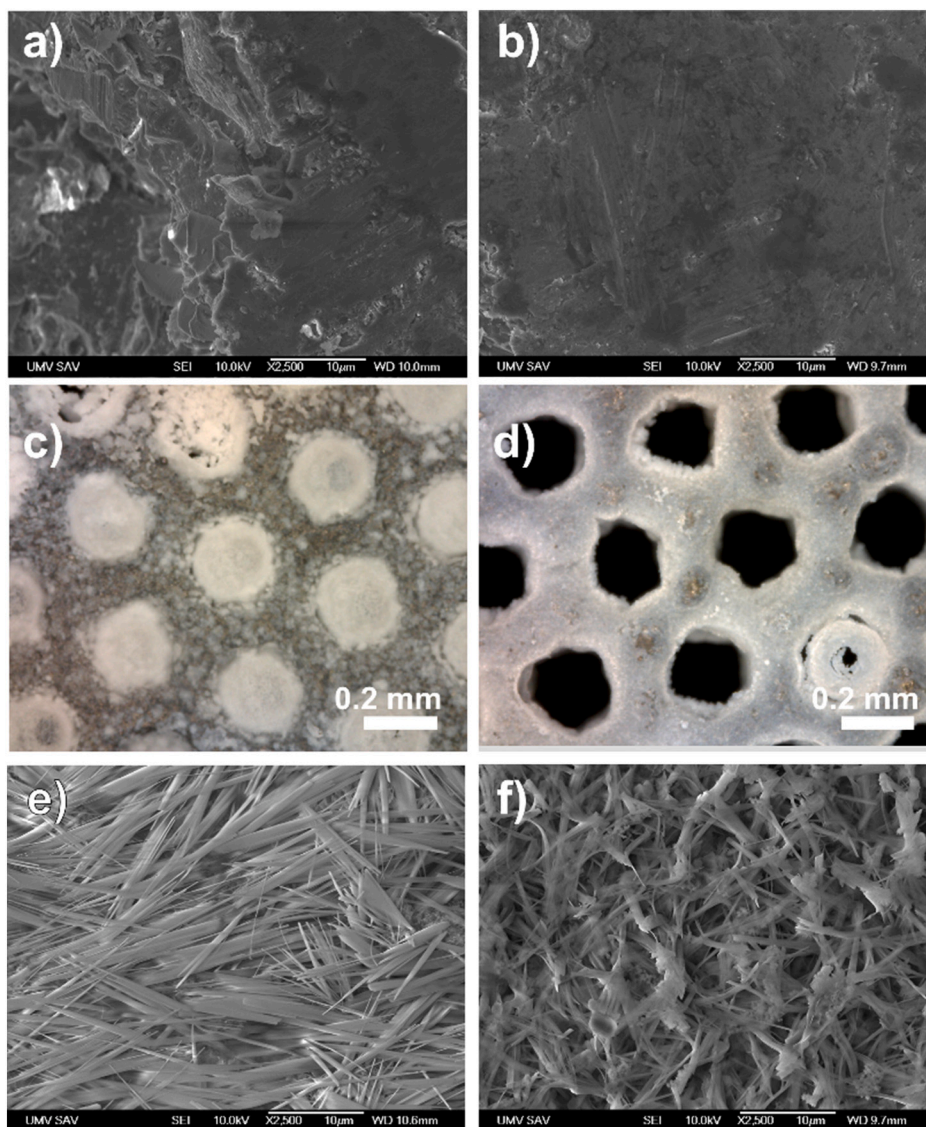


Fig. 7. SEM images of un-annealed (a) and annealed (b) Ti₆Al₄V specimens under 2500× magnification before coating. Representative optical images of specimens with a pore size of 400 µm at 250× magnification after coating with a HAP layer: (c) un-annealed, (d) annealed Ti₆Al₄V alloys. SEM images of un-annealed (e) and annealed (f) Ti₆Al₄V alloys under 2500× magnification after coating with HAP.

nanocrystalline form of HAP was confirmed, while the highest intensity was observed with the specimen fabricated by the O4 procedure. Both α and β Ti phases were observed in the metallic sample. The obtained data correlate with the data published in the literature [28,37].

The chemical composition and distribution of the deposited coating were also examined by an EDX analysis. A comparison of the specimens fabricated by applying O1 and O4 methods (Fig. 6a and d) revealed a difference in the distribution of the deposited coatings. In particular, on the specimen prepared by the O4 method, the coating covered a larger area of the surface of the titanium specimen.

Even though a deposited HAP coating was also confirmed on the specimens fabricated by the O2 method (Fig. 6b), based on previous macroscopic and SEM analyses this particular procedure was evaluated as unsuitable because of the uneven nature of the prepared coating. The EDX analysis revealed the surface distribution and content of individual elements present in the ceramic coating (calcium, oxygen, and phosphorus). For the specimens coated by the O3 method (Fig. 6c), the EDX analysis did not confirm the presence of a HAP coating, and this method was therefore also evaluated as inappropriate. The EDX analysis of the specimens fabricated by the O4 method confirmed the presence of

elements that corresponded to the HAP coating. In all cases, except for the O4 method, the spectra of elements that corresponded to the original Ti₆Al₄V alloy were observed. Their absence or a very weak signal in the specimens prepared by the O4 method (Fig. 6d) confirmed the excess and uniform distribution of the ceramic layer, which caused the signal suppression.

3.3. A comparison of morphology, physical and chemical properties of coatings deposited onto annealed and un-annealed specimens

The processes of evaluation and optimization of the coating methods that were used for the deposition of the coating layer onto the surface of un-annealed specimens were followed by the coating process and the examination of the annealed Ti₆Al₄V specimens. The annealed specimens were coated by applying the O4 method as it was selected in the optimization process as the most appropriate technique. Subsequently, differences in the properties of the surface of the coated annealed and coated un-annealed specimens were studied and compared.

SEM and optical microscopy were used to compare the morphology of the surface of the un-annealed and annealed uncoated specimens

Table 3

Average weights of the annealed and un-annealed specimens with and without a HAp coating, and the corresponding weights of the deposited HAp (number of replicates: $n = 3$).

Annealed specimens coated (O4)	Before coating (g)	After coating (g)	Weight of deposited HAp (g)
400 μm	1.2240 \pm 0.0021	1.2398 \pm 0.0042	0.0158 \pm 0.0137
600 μm	1.3088 \pm 0.0014	1.3189 \pm 0.0037	0.0101 \pm 0.0098
Un-annealed specimens coated (O4)	Before coating (g)	After coating (g)	Weight of deposited HAp (g)
400 μm	1.2538 \pm 0.0011	1.2699 \pm 0.0029	0.0161 \pm 0.0122
600 μm	1.2857 \pm 0.0019	1.2983 \pm 0.0033	0.0126 \pm 0.063

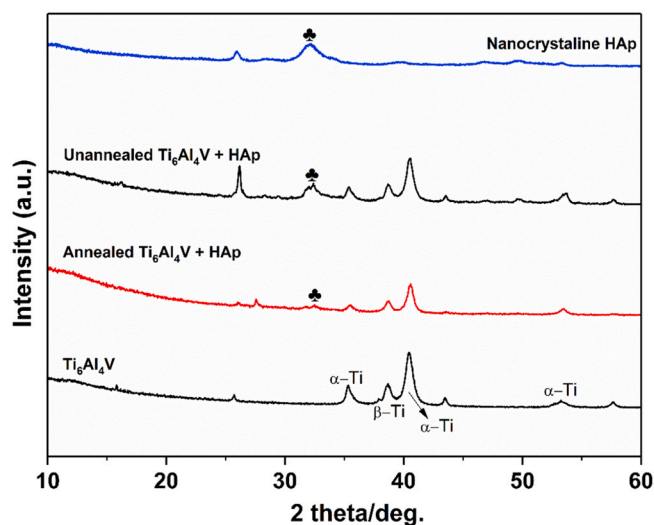


Fig. 8. XRD analysis of the un-annealed and annealed $\text{Ti}_6\text{Al}_4\text{V}$ specimens electrochemically coated with a HAp layer.

(Fig. 7a and b). The annealed Ti specimens exhibited more compact surfaces than the un-annealed Ti specimens, whereas the un-annealed specimens had inhomogeneous, rough surfaces before they were modified by coating with a ceramic layer (Fig. 7a). This may be attributed to the fact that in the process of Ti alloy annealing at high temperatures, the material becomes denser and its surface more compact.

After the coating process, the un-annealed specimens exhibited evenly deposited HAp coatings, which also filled the pores of the examined material (Fig. 7c). Even though the deposited HAp layer was thick, the pores of the annealed alloy were not filled with HAp and remained open (Fig. 7d). In both cases, the ceramic layers had a crystalline microstructure. In the case of the un-annealed specimens (Fig. 7e), the deposited crystals were longer and spindle-like shaped, whereas the annealed specimens (Fig. 6f) were covered by shorter and thicker crystals with flake-like HAp formations on their ends.

To compare the amounts of HAp deposited on the surface of the annealed and un-annealed specimens, the specimens were weighed before and after the coating procedure. The average weights of the individual types of specimens are listed in Table 3. The difference in the weights of the coatings deposited on the annealed/un-annealed specimens was minimal. It may be seen that the un-annealed Ti specimens were coated with a larger amount of ceramic HAp than the annealed specimens which corresponds to the fact that in this case the HAp was also deposited in the pores of the specimens. With a pore size of 400 μm , the differences between the annealed and un-annealed specimens were negligible, whereas with a pore size of 600 μm the average weight of the

deposited coating was higher. It was also observed that the weights of the un-annealed uncoated Ti specimens were higher than those of the annealed uncoated specimens. The difference in the weights might have been caused by the annealing process, during which the structure of the $\text{Ti}_6\text{Al}_4\text{V}$ alloy surface changed.

The XRD analysis confirmed that nanocrystalline HAp was deposited on the un-annealed as well as annealed specimens (Fig. 8). The intensity of the deposited coating was higher on the un-annealed specimens which may be related to the lower crystallinity of the HAp coating observed on the annealed specimens, as proved by the SEM analysis.

The EDX analysis of the annealed specimens also confirmed the presence of phosphorus, oxygen, and calcium (Fig. 9a). The coating was deposited evenly and covered the entire surface of the examined annealed coated specimens (Fig. 9b and c).

The application of ceramic coatings on the same type of titanium alloy as the one in our experiments has been investigated by several research teams. Electrochemical deposition of hydroxyapatite on the surface of structures with larger pores, is, however, not extensively studied. Durdu et al. [38] fabricated and characterized a hydroxyapatite-coated $\text{Ti}_6\text{Al}_4\text{V}$ substrate prepared by the plasmatic electrolytic oxidation (PEO) method. Unlike our experiment, in which we observed a crystalline structure, they produced the amorphous HAp phase, the formation of which they explained by rapid solidification in the very first stages of the PEO processes. Mavis et al. [39] chose the dip-coating method using a HAp suspension and several organic additives. The resulting HAp layer, obtained after calcification, was porous and consisted of spherical particles with an average size of approximately 0.25 μm with a morphology that was different from the morphology of layers produced by electrochemical deposition performed in this study. Morphology of the prepared HAp layer that was like that observed in [39] was also achieved by Alksakal, who prepared a HAp coating by the sol-gel method [40].

Regarding the electrochemical deposition, several authors have observed the morphology of the deposited coating that was similar to that observed in our experiments. Wang [41] prepared HAp coatings by electrochemical deposition in the potentiostatic mode with a potential of -1.4 V vs. SCE. When compared to the potential of -0.8 V, which was used for our specimens in the O3 method, Wang used a more negative potential which is why he achieved the deposition of plate-like crystalline HAp. HAp coating has been electrochemically deposited in several other studies [42–44]. However, when compared to the design of our experiment, the coatings were mostly deposited onto planar, non-porous substrates.

The influence of the type of procedure of hydroxyapatite coating preparation on the titanium structure plays a significant role [45–47]. The electrochemical methods of coating HAp on titanium scaffolds or structures resonates in the scientific sphere [48,49]. However, even with this coating method, there are several factors that have not yet been explored. For example, a study by Kuo et al. [50] where the process of electrochemical deposition of HAp on biomedical titanium at room temperature is described. In this case, HAp coatings were directly deposited on titanium at room temperature. Another difference in the methodology is the fact that the samples were annealed at a temperature of 700 $^{\circ}\text{C}$. In our case, coating deposition is carried out at a temperature of 65 $^{\circ}\text{C}$ and after annealing at 820 $^{\circ}\text{C}$. A similar study in different parameters while maintaining the same methodology was performed by Wang et al. [51] where they describe the coating of HAp on titanium using an electrochemical technique. During coating, they used different concentrations of fluoride ions in the apatite structure originating from the NaF in the electrolyte. In our case, 1 ml/l of 35 % hydrogen peroxide was added to the electrolyte. According to Vladescu et al. [52] the properties of HAp obtained by electrochemical deposition depend on several factors such as deposition temperatures, electrolyte pH and concentrations, as well as the applied potential. Based on this knowledge, it is necessary to determine all possible parameter variations for detection and determination of the most suitable parameters for a given

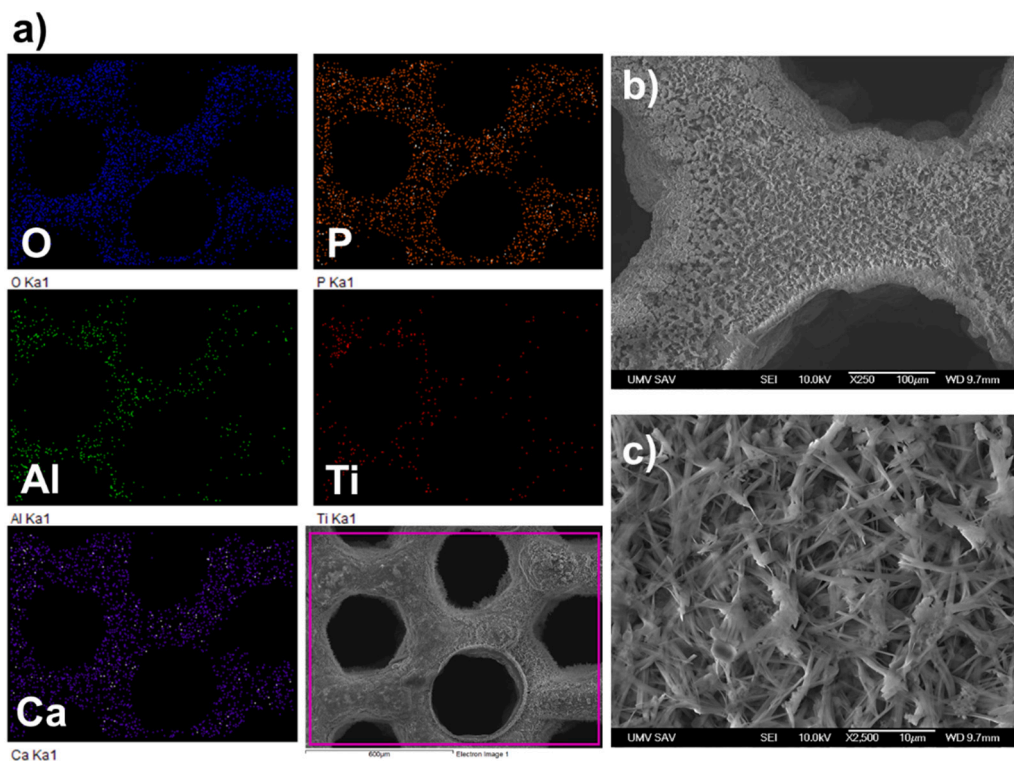


Fig. 9. EDX surface analysis of the annealed specimens electrochemically coated with a ceramic HAp layer by the O4 method (a). SEM images of the surface of the annealed coated specimens under 250× (b) and 2500× (c) magnification.

HAp coating method on the surface structure of titanium and its alloys.

4. Conclusions

Titanium and Ti-based alloys are currently largely used in implantology. This study aimed to identify an optimal method for applying ceramic hydroxyapatite coating onto the surface of titanium specimens with a porous structure, which is intended to be used as bone implants in the future. Moreover, we wanted to compare the nature of the electrochemically deposited Hap layer on the annealed and not heat-treated Ti samples.

Specimens with a porous structure (with a pore size of 200 μm, 400 μm, and 600 μm) were designed and additively manufactured using the SLS method. Following the fabrication process, some of the specimens have been further annealed. Titanium specimens were coated with hydroxyapatite using electrochemical deposition. The un-annealed specimens were used to test several experimental procedures that were subsequently analyzed. Before the coating process, the specimens were cleaned, and some of them were etched to increase the roughness of their surface. The method that was identified as the most appropriate for the application of ceramic coating was electrochemical deposition in the galvanostatic mode with a constant current of 5 mA for 40 min at a temperature of 65 ± 0.5 °C. The surface morphologies of the annealed, as well as un-annealed specimens with HAp coating, were studied and compared. The morphology of the ceramic coating applied to the un-annealed specimens was different from that of the coating applied to the annealed specimens. There were differences both in shapes and distribution of HAp crystals on the surface of the Ti-HAp specimens. Furthermore, an XRD analysis confirmed that the surface of the un-annealed specimens was covered with a higher amount of nanocrystalline HAp than the surface of the un-annealed specimens which may have been caused by higher surface roughness of the un-annealed specimens before coating. In addition, the pores of the annealed specimens were not filled which may have a negative effect on the rate of osseointegration on the surface of such material.

For the future application of these specimens in implantology, it is necessary to further optimize their elastic modulus. The specimens should be therefore subjected to mechanical testing to optimize their porous structure for a particular application area. It is also necessary to conduct testing of the biological compatibility of the fabricated materials.

CRediT authorship contribution statement

Radka Gorejová: Writing – original draft, Writing – review & editing, Methodology, Investigation. **Renáta Oriňáková:** Writing – review & editing, Funding acquisition, Conceptualization. **Zuzana Orságová Králová:** Investigation, Visualization. **Tibor Sopčák:** Investigation, Visualization. **Ivana Šišoláková:** Investigation. **Marek Schnitzer:** Writing – review & editing, Supervision, Validation. **Miroslav Kohan:** Writing – original draft, Writing – review & editing, Investigation, Visualization. **Radovan Hudák:** Funding acquisition, Conceptualization, Supervision.

Declaration of competing interest

The authors declare that they have no known competing financial interests or personal relationships that could have appeared to influence the work reported in this paper.

Data availability

Data will be made available on request.

Acknowledgment

This paper was prepared with the support of the Slovak Research and Development Agency (project APVV-20-0278) and the Ministry of Education, Youth and Sports of the Czech Republic (DKRVO RP/CPS/2022/005). This publication is the result of the project implementation

CEMBAM - Center for Medical Bioadditive Research and Production, ITMS2014+: 313011 V358 supported by the Operational Programme Integrated Infrastructure funded by the European Regional Development Fund.

References

- Jayanthi Parthasarathy, et al., Mechanical evaluation of porous titanium (Ti6Al4V) structures with electron beam melting (EBM), *Journal of the mechanical behavior of biomedical materials* 3.3 (2010) 249–259.
- Mihaela Claudia Spataru, et al., In-depth assessment of new Ti-based biocompatible materials, *Materials Chemistry and Physics* 258 (2021), 123959.
- Lunguo Xia, et al., In situ modulation of crystallinity and nano-structures to enhance the stability and osseointegration of hydroxyapatite coatings on Ti-6Al-4V implants, *Chemical Engineering Journal* 347 (2018) 711–720.
- Jiayi Li, et al., 3D printed dual-functional biomaterial with self-assembly micro-nano surface and enriched nano argentum for antibacterial and bone regeneration, *Applied Materials Today* 17 (2019) 206–215.
- Xiaojian Wang, et al., Topological design and additive manufacturing of porous metals for bone scaffolds and orthopaedic implants: a review, *Biomaterials* 83 (2016) 127–141.
- Ari I. Itälä, et al., Pore diameter of more than 100 µm is not requisite for bone ingrowth in rabbits, *Journal of Biomedical Materials Research: An Official Journal of The Society for Biomaterials, The Japanese Society for Biomaterials, and The Australian Society for Biomaterials and the Korean Society for Biomaterials* 58.6 (2001) 679–683.
- Volker Weißmann, et al., Influence of the structural orientation on the mechanical properties of selective laser melted Ti6Al4V open-porous scaffolds, *Materials & Design* 95 (2016) 188–197.
- Gianluca Turco, et al., Three-dimensional bone substitutes for oral and maxillofacial surgery: biological and structural characterization, *Journal of Functional Biomaterials* 9.4 (2018) 62.
- Ryszard Uklejewski, et al., Structural-geometric functionalization of the additively manufactured prototype of biomimetic multispired connecting ti-alloy scaffold for entirely noncemented resurfacing arthroplasty endoprostheses, *Applied Bionics and Biomechanics* 2017 (2017).
- Lawrence E. Murr, et al., Next-generation biomedical implants using additive manufacturing of complex, cellular and functional mesh arrays, *Philosophical Transactions of the Royal Society A: Mathematical, Physical and Engineering Sciences* 368 (2010) 1999–2032.
- Huanlong Li, et al., Effects of pore morphology and bone ingrowth on mechanical properties of microporous titanium as an orthopaedic implant material, *Materials Transactions* 45.4 (2004) 1124–1131.
- Xiao Bai, et al., Deposition and investigation of functionally graded calcium phosphate coatings on titanium, *Acta biomaterialia* (5.9) (2009) 3563–3572.
- A. Siddharthan, Sampath T.S. Kumar, S.K. Seshadri, *Bioceramics coating on Ti-6Al-4V alloy by microwave processing*, *Surface engineering* 23.6 (2007) 401–405.
- Toshihiro Kasuga, et al., Enhancing effect of autoclogging on bioactivity of β-titanium alloy coated with calcium phosphate glass-ceramic, in: *Key Engineering Materials*, Trans Tech Publications Ltd, 2005, pp. 243–246.
- Patrik Prachár, et al., Cytocompatibility of implants coated with titanium nitride and zirconium nitride, *Bratislavské lekárske listy* 116.3 (2015) 154–156.
- Toshihiro Kasuga, et al., Calcium phosphate invert glass-ceramic coatings joined by self-development of compositionally gradient layers on a titanium alloy, *Biomaterials* 22.6 (2001) 577–582.
- Yu-peng Lo, et al., Cross-sectional analysis on microstructure of plasma-sprayed HA + TiO₂ composite coatings on titanium substrate, *Transactions of the Nonferrous Metals Society of China* 14.6 (2004) 1139–1144.
- Hae-Won Kim, et al., Hydroxyapatite coating on titanium substrate with titania buffer layer processed by sol-gel method, *Biomaterials* 25 (13) (2004) 2533–2538.
- Laila Damiati, et al., Impact of surface topography and coating on osteogenesis and bacterial attachment on titanium implants, *Journal of Tissue Engineering* 9 (2018), 2041731418790694.
- Lai-Chang Zhang, Liang-Yu Chen, Liqiang Wang, *Surface modification of titanium and titanium alloys: technologies, developments, and future interests*, *Advanced Engineering Materials* 22 (5) (2020), 1901258.
- Dongxu Ke, et al., Compositionally graded doped hydroxyapatite coating on titanium using laser and plasma spray deposition for bone implants, *Acta Biomaterialia* 84 (2019) 414–423.
- Naoya Taniguchi, et al., Effect of pore size on bone ingrowth into porous titanium implants fabricated by additive manufacturing: an in vivo experiment, *Mater. Sci. Eng. C* 59 (2016) 690–701.
- Jia Ping Li, et al., Porous Ti6Al4V scaffold directly fabricating by rapid prototyping: preparation and in vitro experiment, *Biomaterials* 27 (8) (2006) 1223–1235.
- Yoshinori Kuboki, Qiming Jin, Hiroko Takita, *Geometry of carriers controlling phenotypic expression in BMP-induced osteogenesis and chondrogenesis*, *JBJS* 83 (1_suppl_2) (2001) S105–S115.
- R. Orinakova, A. Orinak, M. Kupková, M. Hrubovcakova, L. Skantarova, T. A. Morovska, H.F. Arlinghaus, *Study of electrochemical deposition and degradation of hydroxyapatite coated iron biomaterials*, *Int. J. Electrochem. Sci.* 10 (2015) 659–670.
- Mir Saman Safavi, et al., *Electrodeposited hydroxyapatite-based biocoatings: recent progress and future challenges*, *Coatings* 11.1 (2021) 110.
- Xing-yu Chen, et al., Pulsed electrodeposition of hydroxyapatite on titanium substrate in solution containing hydrogen peroxide, *Transactions of Nonferrous Metals Society of China* 17.3 (2007) 617–621.
- Norberto Roveri, et al., Surface enamel remineralization: biomimetic apatite nanocrystals and fluoride ions different effects, *Journal of Nanomaterials* 2009 (2009).
- Khurram Shahzad Munir, Yuncang Li, Cuie Wen, *Metallic scaffolds manufactured by selective laser melting for biomedical applications*, in: *Metallic Foam Bone*, Woodhead Publishing, 2017, pp. 1–23.
- Yingying Du, *Selective laser sintering scaffold with hierarchical architecture and gradient composition for osteochondral repair in rabbits*, *Biomaterials* 137 (2017) 37–48.
- K.F. Leong, C.M. Cheah, C.K. Chua, *Solid freeform fabrication of three-dimensional scaffolds for engineering replacement tissues and organs*, *Biomaterials* 24 (13) (2003) 2363–2378.
- J.-P. Kruth, et al., Binding mechanisms in selective laser sintering and selective laser melting, *Rapid prototyping journal* 11 (1) (2005) 26–36.
- Ben Vandenbroucke, Jean-Pierre Kruth, *Selective laser melting of biocompatible metals for rapid manufacturing of medical parts*, *Rapid Prototyping Journal* 13 (4) (2007) 196–203.
- Dirk A. Hollander, et al., Structural, mechanical and in vitro characterization of individually structured Ti-6Al-4V produced by direct laser forming, *Biomaterials* 27.7 (2006) 955–963.
- Yihan Liu, et al., Evaluation of mechanical properties and porcelain bonded strength of nickel–chromium dental alloy fabricated by laser rapid forming, *Lasers in medical science* 25.6 (2010) 799–804.
- Ting Zhang, et al., Chitosan/hydroxyapatite composite coatings on porous Ti6Al4V titanium implants: in vitro and in vivo studies, *Journal of Periodontal & Implant Science* 50.6 (2020) 392.
- Artur R. Shugurov, et al., Recovery of scratch grooves in Ti-6Al-4V alloy caused by reversible phase transformations, *Metals* 10.10 (2020) 1332.
- Salih Durdu, et al., Characterization and formation of hydroxyapatite on Ti6Al4V coated by plasma electrolytic oxidation, *Journal of Alloys and Compounds* 551 (2013) 422–429.
- Bora Mavis, A.Cüneyt Taş, *Dip coating of calcium hydroxyapatite on Ti-6Al-4V substrates*, *Journal of the American Ceramic Society* 83.4 (2000) 989–991.
- Bünyamin Aksakal, Mehmet Gavgali, Burak Dikici, *The effect of coating thickness on corrosion resistance of hydroxyapatite coated Ti6Al4V and 316L SS implants*, *Journal of materials engineering and performance* 19.6 (2010) 894–899.
- Hao Wang, et al., Early bone apposition in vivo on plasma-sprayed and electrochemically deposited hydroxyapatite coatings on titanium alloy, *Biomaterials* 27.23 (2006) 4192–4203.
- Huei Yu Huang, *Effect of hydroxyapatite formation on titanium surface with bone morphogenetic protein-2 loading through electrochemical deposition on MG-63 cells*, *Materials* 11.10 (2018) 1897.
- Magdalena Łukaszewska-Kuska, et al., Hydroxyapatite coating on titanium endosseous implants for improved osseointegration: physical and chemical considerations, *Advances in clinical and experimental medicine: official organ Wrocław Medical University* 27.8 (2018) 1055–1059.
- Alexandra Ioana Bucur, Emanoil Linul, Bogdan-Ovidiu Taranu, *Hydroxyapatite coatings on Ti substrates by simultaneous precipitation and electrodeposition*, *Applied Surface Science* 527 (2020), 146820.
- Itishree Ratha, et al., Effect of doping in hydroxyapatite as coating material on biomedical implants by plasma spraying method: a review, *Ceramics International* 47.4 (2021) 4426–4445.
- M.P. Ferraz, F.J. Monteiro, C.M. Manuel, *Hydroxyapatite nanoparticles: a review of preparation methodologies*, *J. Appl. Biomater. Biomech.* 2 (2) (2004) 74–80.
- Mohsen Ebrahimi, et al., Taguchi design for optimization of structural and mechanical properties of hydroxyapatite-alumina-titanium nanocomposite, *Ceramics International* 45.8 (2019) 10097–10105.
- Yuan-yuan Zhang, et al., Electrochemical deposition of hydroxyapatite coatings on titanium, *Transactions of Nonferrous Metals Society of China* (16.3) (2006) 633–637.
- Haixin Zhao, et al., The structural and biological properties of hydroxyapatite-modified titanate nanowire scaffolds, *Biomaterials* 32.25 (2011) 5837–5846.
- M.C. Kuo, S.K. Yen, *The process of electrochemically deposited hydroxyapatite coatings on biomedical titanium at room temperature*, *Mater. Sci. Eng. C* 20 (1–2) (2002) 153–160.
- Jian Wang, et al., Fluoridated hydroxyapatite coatings on titanium obtained by electrochemical deposition, *Acta Biomaterialia* 5.5 (2009) 1798–1807.
- Alina Vladescu, et al., Influence of the electrolyte's pH on the properties of electrochemically deposited hydroxyapatite coating on additively manufactured Ti64 alloy, *Scientific reports* (7.1) (2017) 1–20.